

Development of instrumentation and methods for MAD and structural genomics at the SRS, ESRF, CHESS and Elettra facilities

Alberto Cassetta,^a Ashley M. Deacon,^b Steve E. Ealick,^b John R. Helliwell^{c*} and Andrew W. Thompson^d

^aInstitute of Structural Chemistry, CNR, Rome and Sincrotrone Trieste, Italy, ^bDepartment of Chemistry and Chemical Biology, Cornell University, USA, ^cChemistry Department, University of Manchester, Manchester M13 9PL, UK, and ^dEMBL, Avenue des Martyrs, Grenoble, France. E-mail: john.helliwell@man.ac.uk

(Received 12 March 1999; accepted 4 May 1999)

The evolution of the brilliance of synchrotron radiation sources has allowed combined functionalities of beamline optics for simultaneous high intensity, rapid tunability and narrow wavelength bandpass. This then combines the chance to measure protein crystal diffraction data at multiple wavelengths for optimized anomalous dispersion (MAD) differences for phasing as well as at high diffraction resolution from macromolecular structures and their complexes. Rapid *de novo* protein structure determination is now achieved. The selenomethionine substitution method offers a definite way to incorporate anomalous scattering atoms in a protein for MAD, although MAD is also a very versatile approach applicable to metalloproteins and to cases of many heavy atoms found useful in isomorphous derivative preparation (especially utilization of non-isomorphous derivatives). Detector developments, especially image-plate scanners and now CCDs, have revolutionized diffraction data quality and speed of data acquisition, with further developments, such as the pixel detector, in store. Cryocooling of the sample has greatly alleviated radiation damage problems. Computer hardware capabilities have also changed incredibly. Coordinated software developments for protein crystallography have been achieved [Collaborative Computational Project, Number 4 (1994). *Acta Cryst. D* **50**, 760–763]. Protein crystallography and synchrotron radiation is capable of yielding ‘genome level’ numbers of protein structures. Results and capabilities are presented and summarized, especially from the synchrotron radiation sources and instruments with which the authors have principally been involved, namely SRS, Daresbury and ESRF, Grenoble as well as CHESS, Cornell and Elettra, Trieste. Rapid protein preparation and crystallization remain as major hurdles.

Keywords: protein crystallography; multiwavelength anomalous dispersion (MAD); genomics; proteomics.

1. Introduction

Optimized anomalous scattering, high-resolution and dynamical studies *using synchrotron radiation* were envisaged for protein crystal structure and function determination (*e.g.* see Helliwell, 1979). This could also allow a complete molecular anatomy targeting rational drug design as an important biological application through the knowledge of protein receptor structure (*e.g.* see Helliwell, 1977*a*). This ‘complete molecular anatomy’ is now encapsulated in the terms structural and functional genomics or proteomics. The pace of gene sequencing, from which protein amino acid sequences are derived, has been phenomenal. The pace of three-dimensional protein structure determination is also accelerating quickly,

offering experimental capabilities in structure and function definition on a large numbers scale. Today the Protein Data Bank holds some 9500 protein structures of which some 7800 are derived from protein crystallography. The remainder are derived from NMR solution and electron diffraction structure determination as well as modelling. The number derived from using synchrotron radiation is growing rapidly (Helliwell, 1992; Chayen & Helliwell, 1998). In the future the prediction of protein fold from amino acid sequences may become possible, which will further accelerate the pace of experimental protein structure and function determination.

The development of synchrotron-radiation protein-crystallography beamline instrumentation initially, some 20 years ago, encompassed two separate approaches (high-

intensity optics *versus* rapidly tunable optics; *e.g.* see Helliwell, 1979). A major challenge was how to harness the typical first- and second-generation synchrotron radiation source emittance (source size and divergence) available at that time so as to match the available protein crystal sample acceptance (crystal size and mosaicity). The emittances of synchrotron radiation sources have improved considerably over the years. On a third-generation high-brilliance synchrotron radiation source, rapid tunability, needed for measuring more than one wavelength around an elemental absorption edge to vary the anomalous dispersion signal, can be provided whilst simultaneously having a high-intensity X-ray beam at the sample. The reflection intensities can thereby be measured precisely and accurately.

This article will concentrate on an overview of instrumentation, methods and results from Daresbury, SRS and ESRF, Grenoble as well as Elettra, Trieste and CHESS, Cornell in macromolecular crystallography.

Our article salutes the achievements of Sir John Walker from the MRC Laboratory of Molecular Biology in Cambridge, UK, and his Nobel-Prize-winning investigation on F1ATPase, whose protein crystal structure determination (Abrahams *et al.*, 1994) was derived from data measured on the SRS 'PX' station 9.6 as well as SRS 'PX' station 9.5, both equipped with MAR Research image-plate scanners. The high intensity of the SRS X-ray beam at the F1ATPase crystal sample, along with the beam collimation, were the synchrotron radiation beam properties exploited in that data collection, and phase determination was *via* the isomorphous replacement method (with a degree of optimized anomalous scattering through use of short-wavelength synchrotron radiation).

2. Evolution of synchrotron radiation protein crystallography (PX) instruments

2.1. Daresbury; the first dedicated second-generation synchrotron radiation X-ray source

The Daresbury SRS was the first dedicated synchrotron radiation X-ray source and as such, being non-parasitic, is a second-generation synchrotron radiation source. It came on-line in 1981. The progenitor (predecessor) of the SRS was the NINA first-generation synchrotron radiation source. NINA was closed in 1976 to embark on the construction of the SRS itself. On NINA, an optimized anomalous scattering experiment on a platinum tetracyanide derivative of a 6-phosphogluconate dehydrogenase enzyme crystal showed the need for focusing X-ray optics (Helliwell, 1977*b*). Also in the NINA experimental hall was a focusing camera for fixed-wavelength operation for muscle diffraction; Haslegrove *et al.* (1977) showed that in parasitic high-energy-physics mode NINA source movements degraded the X-ray beam focus and intensity, and proposed a dedicated mode of operation for synchrotron radiation experiments.

The first SRS protein crystallography instrument was station 7.2 on the very first X-ray beamline at SRS. The

station optics (Helliwell *et al.*, 1982) comprises a vertically focusing mirror in 1:1 focusing mode and an oblique-cut focusing monochromator: a single crystal of Ge(111) cut at 10° to the surface. This type of monochromator was introduced originally at LURE (Lemonnier *et al.*, 1978). The SRS bending-magnet beamline 7 source sizes of 0.4 × 14 mm² were thus focused to 0.4 × 1.4 mm² at the sample position, quite a reasonable match to typical sample sizes (at that time) of 0.5 mm cross section. Station 7.2 has served a national and international user community, and is still in service today [with an upgraded image-plate detector rather than the Arndt–Wonacott (1977) oscillation camera used at its inception in 1981]. It allowed the definition of the instrument smearing contributions of, firstly, asymmetric beam cross fire and, secondly, spectral spreads of two types: conventional X-ray source type and a correlated-wavelength-with-horizontal-beam-direction type. The latter could be deliberately set up (a so-called non-Guinier focusing mode of the monochromator) to establish a dispersive setting. Thus a polychromatic profile could be established and centred on an X-ray absorption edge to probe in a continuous way the variation of dispersion coefficients of an element in the diffraction spots. This indicated the scope of optimized anomalous dispersion for phasing in protein crystallography. Data for an *L*_{III} absorption edge of a rhenium compound served as the test case (Arndt *et al.*, 1982). In the collection of protein crystal diffraction data a non-dispersive (Guinier) focusing setting of the monochromator was utilized for which the spectral bandpass was as small as 5 × 10⁻⁴. These Guinier and non-Guinier instrument settings are linked to the prediction of the partiality of reflections in the oscillation camera method (Greenhough & Helliwell, 1982) and subsequent data processing [see, for example, Rossmann (1999) in this issue]. A description of the station and the projects streaming through in the first year of operation, as an example, can be found in Helliwell *et al.* (1982). A survey of all publications submitted by users of the SRS 'PX' stations can be found on the SRS www database (Rizkallah, 1999). High-resolution and MIR-derivative data collection was the basis of user beam time proposals then. However, one of the first structural studies unique to synchrotron radiation was the use of station 7.2 to tune the X-ray wavelength to the Mn *K*-edge in pea lectin crystals (Einspahr *et al.*, 1985). In that experiment the use of two wavelengths (1.488 and 1.86 Å), at 1.8 Å and 2.4 Å diffraction resolution, respectively, showed the variation in the Mn anomalous dispersion and, relative to the neighbouring Ca ion, identified which ion was which for these two elements of similar atomic number (Einspahr *et al.*, 1985).

The SRS had a superconducting wiggler magnet inserted in 1983. This allowed the development of a second PX station but with an order of magnitude higher intensity at wavelengths around 0.9 Å, the critical wavelength of emission of the wiggler (compared with 4 Å for the equivalent parameter on the bending-magnet beamline 7). Station 9.6 came on-line in 1984. The beamline optics again

were tailored to the rather large SRS wiggler source size in the horizontal of ~ 14 mm but with a fine vertical source size of again ~ 0.5 mm. Thus 1:1 focusing in the vertical direction *via* a focusing curved mirror and a 10:1 oblique-cut demagnifying Si(111) monochromator was used (Helliwell *et al.*, 1986). For the first time, anxieties about the X-ray beam power onto the optics, from the wiggler, surfaced. This led to the need to set the mirror at a finer glancing angle than for the station 7.2 mirror to reduce as much as possible the heat absorbed by the mirror, the first optical element in the synchrotron radiation white beam. The direct wiggler white beam could burn a hole in a fluorescent screen. In fact, 0.25 kW power was contained in the 4 mrad fan available to the station. The fine mirror glancing strategy and the mirror bending control (which was now handling several kilometres radius of curvature setting) was successful. The focal spot was 0.5×1.4 mm² at the sample, like on SRS 7.2, in spite of the higher heat load on the optics. The beam was now tunable for wavelengths from 0.5 Å upwards, to around 1.38 Å typically, but concentrating on wavelengths tuned to somewhere in the band 0.9–1.1 Å (Helliwell *et al.*, 1984). The spectral band-pass at the Guinier setting of the monochromator was again $>5 \times 10^{-4}$. Thus, high-atomic-number absorption elements became practicable for optimized anomalous scattering. This was exploited especially with isomorphous replacement derivatives, prepared by users in their home laboratory. The large fan emitted from the wiggler created the floor space to place the sample camera collimator to receive the white-beam polychromatic spectrum. This allowed broad-bandpass synchrotron-radiation Laue protein crystal diffraction patterns to be recorded for the first time (Helliwell, 1984, 1985). The tunable monochromatic beam was also exploited whereby single isomorphous replacement with optimized anomalous scattering (SIROAS) was found to be practicable with a large protein such as glutamate dehydrogenase (Baker *et al.*, 1990). Use of a short-wavelength (0.9 Å) monochromatic beam proved popular in reducing the radiation damage of virus crystals. The choice of 0.90 Å was set to maximize the absorption of the photographic films used in the oscillation film camera used at that time for data collection. The structure determination of the foot-and-mouth-disease virus (FMDV) was based on data measured on station 9.6 (Acharya *et al.*, 1989), as was that of the SV40 virus from Harvard (Liddington *et al.*, 1991). The bulk of proposals on this station were then, firstly, for very large unit-cell data collection from virus crystals (and later from F1ATPase) or, secondly, for MIR/SIR-derivative data collection or, thirdly, for high-resolution data collection. The reduction of absorption errors in the data from the use of short wavelengths improved heavy-atom phasing and protein model refinement. Use of photographic film was tedious and repetitive, as well as noxious. New ground was broken by the introduction of the FAST area TV diffractometer purchased from Enraf–Nonius and which gave a glimpse of the world of on-line image-plate and CCD area detectors

with improved detector quantum efficiency and, by comparison, fantastically automatic data collection. Multiple data-set measurements of many kinds beckoned; multiple wavelengths, multiple time slices, multiple drug lead compound inhibitor data sets *etc.* Radiation damage was less with these more sensitive detectors. Smaller protein crystals would yield complete data sets [*e.g.* see the case of trypanothione reductase whereby Bailey *et al.* (1993) used the FAST diffractometer on station 9.6 in such an application].

Improved brilliance (or brightness) of the SRS came in 1985, whereby the horizontal source size challenges referred to above were greatly alleviated. The need, with the SRS high-brightness lattice, for such a large demagnification of the horizontal source was removed. Obviously the existing stations 7.2 and 9.6 had improved (finer) horizontal foci by a factor of about five. But a new beamline optic became possible whereby the 1:1 focusing of a (toroid) mirror alone would be sufficient for many protein crystal samples and the monochromator need not then have a focusing role. Rapid wavelength tuning (XAFS style) became possible with reasonable intensity on the same station. Rapidly tunable MAD experiments were thus going to be feasible.

A rapidly tunable wiggler station 9.5 design based on a toroid mirror optic and a double-crystal monochromator was made (Brammer *et al.*, 1988). Moreover, the removal of the monochromator would make possible a point-focused white beam of X-rays for 'pink'-beam Laue diffraction with a wavelength range of 0.5 Å upwards to ~ 2 Å. The upper wavelength limit was set by the beryllium absorption in the vacuum line windows. The principal challenge of this optic design is the sensitivity to alignment of the 'yaw' angle of the toroid mirror optic. A vertical focusing curvature of kilometres is readily 'contaminated' by tens of metres in the horizontal if the mirror is misaligned by only tens of arcseconds. The X-ray wiggler power incident on the mirror was analysed by finite-element analysis and ray tracing (Brammer *et al.*, 1988). In fact, the focusing performance and alignment proved straightforward (Thompson *et al.*, 1992). A problem, however, proved to be SRS source movements, which are relatively of the same type as the mirror 'yaw' error. Such movement problems were solved *via* careful SRS source monitoring and thereafter a feedback loop to control the source position. The intensity was a factor of 50 times that of a rotating-anode X-ray home source but a factor of ten below that of stations 7.2 and 9.6. The use of station 9.5 has allowed the development of rapidly tunable MAD experiments at SRS.

Peterson *et al.* (1996) compared phasing success for different combinations of wavelengths and compared different theoretical approaches. Data sets at four wavelengths were measured in 24 h, including the fluorescence scan of the bromine edge for the brominated nucleotide crystal involved. The data were measured at room temperature and so, to minimize the effect of time-dependent damage or source-movement-derived intensity

fluctuations, including beam decay, the data at each wavelength were measured close together in time for contiguous angular wedges of data. The crystal was perfectly aligned to measure Friedel differences across the crystal mounting axis, again minimizing the time difference between Friedel-equivalent reflections (Einspahr *et al.*, 1985; Nieh & Helliwell, 1995). MAD phasing using two (the minimum required), three and four wavelengths were compared. A data set measured at the peak of the white line but with the crystal deliberately mis-set showed the bad effect of this on the phasing quality in the two-wavelength phasing combinations. 40 years of phasing strategies (Okaya & Pepinsky, 1956; Herzenberg & Lau, 1967; Hoppe & Jakubowski, 1975) were compared for synchrotron radiation MAD data for the first time. The use of three wavelengths around the selenium *K* edge of hydroxymethylbilane synthase allowed a *de novo* structure determination of the active form of this enzyme (Hädener *et al.*, 1999). This study utilized CCP4 software treating one of the wavelengths as the native, *i.e.* the point of inflection of the rise of the absorption edge being where the real coefficient of anomalous dispersion is at its minimum and the anomalously scattering atom is rendered a 'light' atom as a result. Glover *et al.* (1995) also used station 9.5 for MAD with the uranyl derivative of OppA and the uranium *L_{III}* edge and data measured at four wavelengths. The kind of experiment envisaged then in the early experiments on NINA (Helliwell, 1977*b*) were brought finally to fruition at Daresbury.

Soon SRS will have two new stations on a new multipole wiggler beamline (Duke *et al.*, 1998). These are of the slow tunable design, like SRS 7.2/9.6. The need for rapid tuning of the wavelength has perhaps eased in that cryocooling of the sample allows whole data sets to be collected with little or no radiation damage. Therefore, time-dependent variations in the measurements are now due to beam-intensity fluctuations alone. There is also a standardization towards the most popular element and absorption edge being selenium (Hendrickson *et al.*, 1990). It should be practical, with this more homogeneous set of conditions, to work with the 'slow tunable' optic design of 7.2/9.6 for Se MAD data collection. The two styles of X-ray optics on the PX stations at SRS are shown in Fig. 1.

The blending of high intensity and rapid tunability on the one beamline became possible with the advent of ESRF, the historical development of which, for macromolecular crystallography, is described in the following section and whose development was closely dependent on the national facilities at *e.g.* SRS and LURE (Helliwell & Fourme, 1983; Helliwell, 1987).

2.2. ESRF; the first third-generation high-brilliance synchrotron radiation X-ray source

Within Europe, community discussions and targeted workshops sought to arrive at a proposal for a European Synchrotron Radiation Project (ESRP). These commenced in 1979 based on a 5 GeV machine with undulators, wigglers and bending magnets as sources. The ESRP was

led by B. Buras and led to the European Science Foundation (ESF) Report in favour of an ESRF. The brilliance [$\text{photons s}^{-1} \text{mm}^{-2} \text{mrad}^{-2} (\delta\lambda/\lambda)^{-1}$] offered from X-ray undulators was staggering. Also, the X-ray beam power from multipole wigglers was huge compared with anything seen previously, reaching up to 10 kW mrad^{-1} , some two orders higher than on the SRS wiggler. There were also concerns about the tolerance of the samples to the very large X-ray beam intensities to become available. Helliwell & Fourme (1983) reported on the thermal and radiation damage blast on a protein crystal and recommended use of shorter wavelengths than standard at that time (*e.g.* 1 and 0.5 Å were considered in detail). Also, thermal analysis of the crystal mount suggested use of a copper stalk and low temperatures to remove the heat. There would be limits to the smallest size of sample that could be studied. These limits were explored down to 20 μm by Hedman *et al.* (1985). Restrictions would also apply to the larger unit cells. However, use of a large number of crystals to make a data set would always be a possible approach. The time-resolved experiments would be time-sliced, however, so that the total heat load on a regular-sized crystal would be kept tolerable. The ESRF machine energy was upgraded during these discussions to 6 GeV to facilitate Mössbauer scattering experiments based on undulator X-ray emission at 0.86 Å wavelength. The tuning range of undulators would also be improved by such an approach. In the first instance the recommendations for beamlines for macromolecular crystallography, after extensive consultation

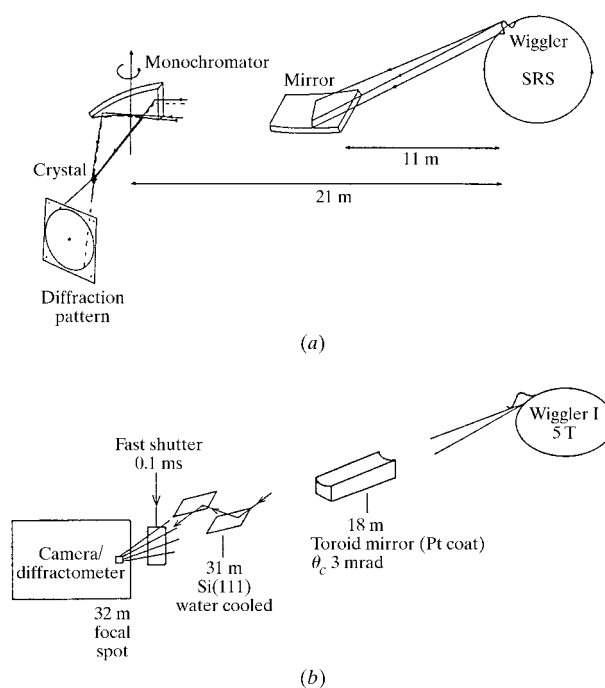


Figure 1

The group of SRS protein crystallography ('PX') stations 7.2, 9.6 and 9.5 (Helliwell *et al.*, 1982, 1986; Brammer *et al.*, 1988), which will be expanded soon to also include two new multipole wiggler PX stations on beamline 14 (Duke *et al.*, 1998), utilize the two generic styles of X-ray optics shown here in (a) and (b).

including *via* the European-wide CCP4 newsletter, were for undulator, multipole wiggler and bending-magnet stations for protein crystallography. These would initially concentrate on large unit cells, time-resolved studies and MAD, respectively. This would allow time for the research and development on high-heat-load monochromators and experience to be gained (including users being allowed to change the undulator gap for tuning applications). Hence, beamlines BL4 (IDO2) undulator, BL3 (IDO9) wiggler (actually a hybrid wiggler/undulator) and BL19 bending magnet (BM14) are running routinely today. The relative performances of the beam brilliances and intensities *versus* the SRS are that, roughly speaking, SRS 9.6 allows studies at medium to high resolution for unit cells up to 500 Å, *e.g.* FMDV (Acharya *et al.*, 1989) and SV40 (Liddington *et al.*, 1991), but ESRF BL4 allows unit cells to be studied to 1000 Å, *e.g.* blue tongue virus (Grimes *et al.*, 1997), and larger. SRS 9.5 in focused white-beam mode allows exposure times into the millisecond range (unfocused the SRS wiggler affords protein crystal Laue exposures into the seconds range) whereas ESRF BL3 has 1000 times shorter exposure, a critical gain factor because that allows exposures to be made from a single circulating ESRF bunch of electrons, with intrinsic time resolution of the bunch width of 60 ps (Bourgeois *et al.*, 1996). ESRF BM14 is an order of magnitude higher than the intensity of the monochromatic SRS 9.5 intensity, thus matching the SRS 9.6 intensity 'slow tunable' station design. Fig. 2 shows the beamline BM14 optics scheme. This is based on the SRS 9.5 approach but with the addition of a collimating pre-mirror. A total of almost 30 MAD-solved protein structures have emanated from BM14 use in 1998 alone (Laboure *et al.*, 1999). There is now a four-hutch undulator beamline 'Quadrigia' (ID14) for macromolecular crystal data collection including a MAD endstation (Wakatsuki *et al.*, 1998). Also, there are two CRG BM beamlines (FIP/D2AM) which include a MAD data-collection capability. A dedicated undulator line (ID29) for MAD is under construction (see §4; Chayen *et al.*, 1996).

2.3. Cornell; CHESS and MacCHESS

The Cornell High Energy Synchrotron Source (CHESS) is a 5.3 GeV synchrotron radiation facility funded by the National Science Foundation. It was established as a first-generation source, due to its parasitic use of the Cornell Electron Storage Ring (CESR), and subsequently pioneered the use of multipole wiggler insertion devices for structural biology. As a result of its continuing use of CESR the beam lifetimes are short, with an average fill length of ~75 min. CHESS maintains the high-intensity X-ray beams, including optical elements, to all ten of the experimental stations, while it is the National Institutes of Health funded MacCHESS research resource that supports the operation of three of these stations for macromolecular crystallography. Two of the stations (A1 and F1) operate as monochromatic X-ray sources, with a fixed wavelength of ~0.92 Å, while the third station, F2, offers a doubly focused X-ray beam with a tunable wavelength in the 0.5–1.8 Å range. Each of these stations receives a 2 mrad fan of radiation from either the A-line or the F-line 24-pole 1.2 T permanent-magnet wigglers.

The first MAD phasing experiment at CHESS was conducted on station F1 (Leahy *et al.*, 1992) with a customized experimental set-up, including a channel-cut monochromator for high-energy resolution. The data were collected on Fuji imaging plates at 277 K and, as a result, three crystals were required to complete a four-wavelength MAD experiment. The essential instrumentation for conducting a MAD experiment was subsequently installed on the F2 station and soon thereafter the first successes were reported. In particular, the structure of the restriction endonuclease BamHI (Newman *et al.*, 1994) was determined from a three-wavelength MAD dataset collected from five crystals at 278 K. At this time the benefits of cryogenic data collection (Hope, 1988), in conjunction with a novel crystal mounting technique developed at CHESS (Teng, 1990), were becoming essential to the success of crystallographic projects that exploited the intense X-ray

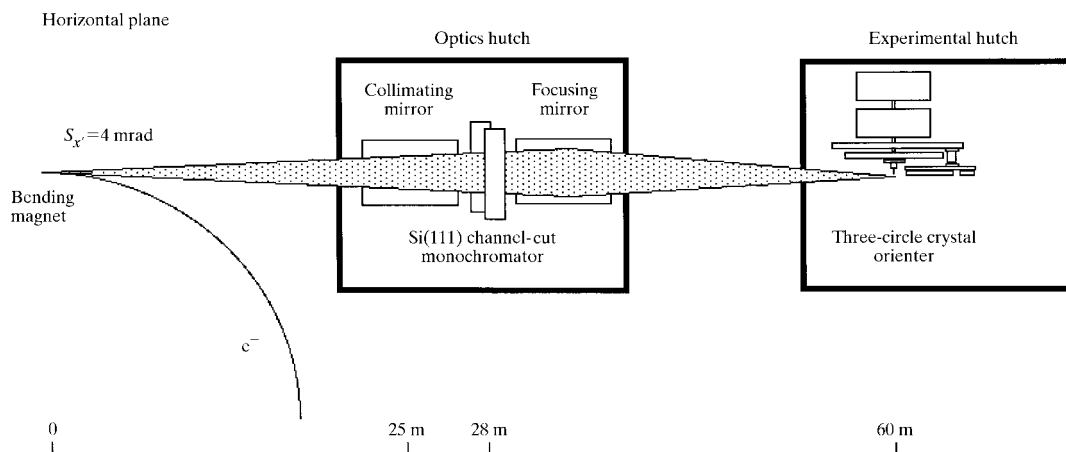


Figure 2 ESRF MAD beamline (BL19/BM14) optics scheme, which is of the SRS 9.5 type (Fig. 1*b*), with the addition of a 'collimating' pre-mirror.

Table 1
Evolution of detectors used for MAD phasing at CHESS.

| Detector | Year | Active area | No. of pixels | Readout time (s) |
|--------------------|------|-----------------|---------------|------------------|
| Fuji images plates | 1992 | 200 mm × 250 mm | 2048 × 2560 | 90† |
| Princeton 1k CCD | 1993 | 51 mm × 51 mm | 1024 × 1024 | 20 |
| 2k CCD | 1994 | 82 mm × 82 mm | 2048 × 2048‡ | 7‡ |
| Quantum 1 | 1995 | 82 mm × 82 mm | 1152 × 1152 | 10 |
| Quantum 4 | 1997 | 188 mm × 188 mm | 2304 × 2304 | 10 |

† Plates scanned offline, with an additional 7 min erase time per plate. ‡ CCD frequently operated in binned 1024 × 1024 mode with 2 s readout.

beams. These techniques were further improved and developed by CHESS users (Rodgers, 1994) and soon started to have an impact on MAD phasing. The datasets used in the structure determinations of the lac repressor core tetramer (Friedman *et al.*, 1995) and the single-stranded DNA binding protein gp32 from T4 bacteriophage (Shamoo *et al.*, 1995) were both collected from single crystals flash frozen at 103 K. At this time user demand resulted in less than 50% of the available F2 time being scheduled for MAD phasing experiments. However, these early demonstrations of the F2 MAD phasing capability, coupled with the popularization of cryocrystallography techniques, encouraged a rapid increase in the number of requests for this facility. The development of MAD phasing at CHESS has also been intimately linked with the pioneering development of CCD detectors for macromolecular crystallography (in collaboration with Sol Gruner, formerly of Princeton University and now Director of CHESS). It is the rapid duty cycle of these detectors, realising efficient use of synchrotron beam time, that has allowed the increasing demand for MAD phasing to be met. The evolution of detectors that have been used for MAD phasing at CHESS is summarized in Table 1. In 1993 the first CCD detector, known as the 'Princeton 1k CCD', was installed at CHESS (Tate *et al.*, 1995). It was based on a 1k CCD chip and had an active area of just 51 mm × 51 mm. Nevertheless, the detector sensitivity and fast readout time, of 20 s, coupled with its small pixel size, allowed efficient data collection from macromolecules and it immediately proved to be a valuable tool for MAD phasing (Fig. 3). During its initial commissioning period it was used in the MAD structure determination of rusticyanin (Walter *et al.*, 1996) and interferon- γ receptor complexed with interferon- γ , a 120 kDa protein complex determined from the anomalous scattering of six selenomethionine residues (Thiel *et al.*, 1995). As the detector began its first period of full user operation it was used in the structure determination of avian-sarcoma virus integrase (Bujacz *et al.*, 1995). The detector also found application, on other beamlines, in a wide variety of high-resolution structure determinations (Walter *et al.*, 1995) and ultrahigh-resolution data collection was initiated (Deacon *et al.*, 1995, 1997). With the success of the 1k CCD firmly established, another device, this time based on a 2k CCD chip, was developed in collaboration with Princeton Scientific

Instruments. This detector offered an increase of ~ 2.6 times in active area and a reduction in readout time to ~ 7 s. The first commissioning results using this detector highlighted its benefit in challenging crystallographic projects (Thiel *et al.*, 1996). This was quickly followed by the purchase of an ADSC Quantum 1 detector. This non-commercial prototype detector from ADSC was based, in part, on the earlier detectors used at CHESS. It offered a similar active area to the 2k CCD, although it was based on a 1k CCD chip. This detector system also featured a user-friendly graphical control interface running on a UNIX workstation (Szebenyi *et al.*, 1997). By this stage in 1996 the demand for MAD phasing time was far in excess of the scheduled time (amounting to an approximately 50% share of the total F2 time). In the same year the X-ray optics on the F2 station were upgraded with an internally cooled monochromator (Smolenski *et al.*, 1997). The increased thermal stability offered by this design, in the face of ever-increasing CESR beam currents, realised an order of magnitude increase in intensity for F2 experiments and thereby decreased exposure times by a similar factor. The rapid duty cycle of the fast-readout CCD detectors was now being fully exploited. By 1997 MAD phasing was accounting for about 80% of the available time on F2. At this point the station became fully configured for MAD phasing, with a complete redesign of the oscillation camera (Thiel *et al.*, 1998) and the installation of a mosaic 2 × 2 ADSC Quantum 4 CCD detector. Since that time there has

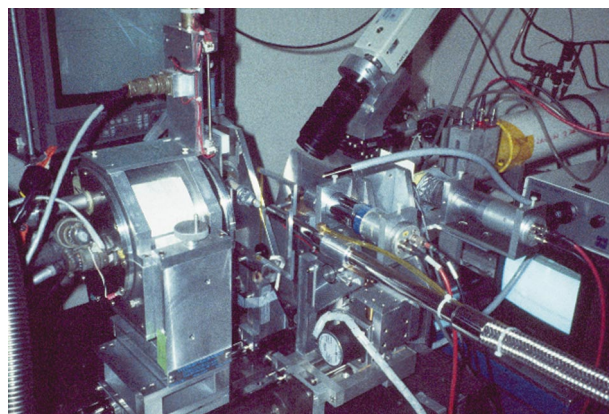


Figure 3
CCD ('Princeton 1k' prototype) detector installed at CHESS on station F2 (Tate *et al.*, 1995).

Table 2

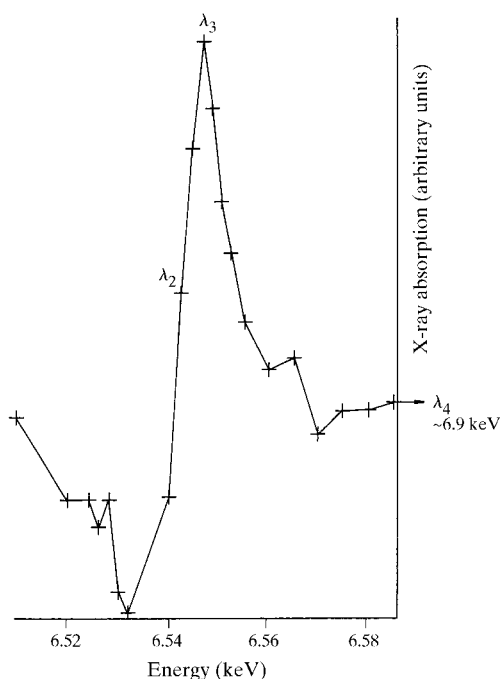
Example of a machine insertion device and MAD beamline; the XRD beamline at Elettra.

| | |
|------------------------|----------------------------------|
| Multipole wiggler | NdFeB hybrid |
| Number of poles | 57 |
| Gap | 22 mm |
| Critical energy | 4.2 keV |
| Useful range | 4–20 keV |
| Monochromator | Double-crystal Si(111)/Si(220) |
| Mirror | Three-segment Pt-coated toroidal |
| Detector | Mar 345 imaging plane |
| Elettra machine energy | 2 GeV |

been a remarkable increase at CHESS in both the efficiency of typical MAD data collection and in the size of structure that can be studied.

2.4. Elettra, Trieste; third-generation 2 GeV synchrotron radiation high-brilliance X-ray source

The Elettra project started in 1987, with the aim to create in Trieste a third-generation machine for the Italian synchrotron radiation community. The machine was intended mainly as a soft X-ray facility (and therefore complementary to ESRF), with a ring energy in the 1.5–2.0 GeV range and a very low emittance, in order to deliver an X-ray beam of very high brilliance. The machine has been operational since 1993, reaching the specification of the original project. Today the machine is working mostly at 2.0 GeV in multibunch mode (with a circulating current of 300 mA after injection). In 1998 the machine was tested at 2.4 GeV and 150 mA, and several shifts in this mode are

**Figure 4**

Fluorescence spectrum recorded for the Mn *K* edge at Elettra in a three-wavelength study for 25 kDa concanavalin A (Hunter *et al.*, 1999; Kalb *et al.*, 1999). (Reproduced with permission from *Croatia Chemica Acta*.)

planned in the future. Even if the Elettra machine was intended mostly for the soft X-ray region, an X-ray crystallography multipole wiggler beamline was also approved and funded, as a joint agreement, from Sincrotrone Trieste and the Italian National Council of Research (CNR). The ‘XRD’ beamline is fed from a three-section multipole wiggler (Table 2), the monochromator is an Si(111) or Si(220) double crystal (wavelength range from 3.0 to 0.5 Å), and the beam is focused from a toroidal mirror (Bernstorff, Busetto, Gramaccioni *et al.*, 1995; Bernstorff, Busetto, Savoia *et al.*, 1995). The beamline has been improved over the years in order to fully exploit the power of the 57 multipole wiggler. Recently a new and better cooled first crystal increased the stability of the X-ray beam and its intensity. The first detector was a MarResearch 180 mm device, which was replaced by a MarResearch 345 mm device in 1997, allowing a much more flexible data acquisition. A CCD detector, to be mounted on a four-circle diffractometer, is also planned. The beamline construction started at the beginning of 1994, and the first diffraction image was obtained in the summer of the same year. The beamline was fully operational from 1995 and has proved very popular across Europe for PX data and includes MAD applications. Todd *et al.* (1999) report a Br-oligonucleotide MAD study. Hunter *et al.* (1999) report an Mn *K*-edge MAD study of native concanavalin A, one of the longest-wavelength MAD studies conducted to date (Fig. 4). Indeed, since a large fraction of proteins are intrinsically metalloproteins (see Hasnain & Hodgson, 1999), the flexibility of a beamline to reach a wide range of X-ray wavelengths is important. There is also new MAD inorganic chemical crystallography whereby for CoZnAPO a five-wavelength study has been undertaken at the two *K* edges (for cobalt and zinc) and midway between (Helliwell *et al.*, 1999). Due to the large demand of beam time for the XRD station, Sincrotrone Trieste has proposed a second XRD beamline, also from a multipole wiggler.

This detailed survey of the stations at SRS, ESRF, CHESS and Elettra indicates the growing surge of PX station developments in these facilities. There are also major station/instrument installations at another ten or so facilities worldwide [for a survey of facilities for synchrotron radiation PX, see Helliwell (1998)]. This is a major technical capability that has sprung up in little over 20 years. Synchrotron radiation machine brilliance has also improved dramatically in the same period.

3. Locating multiple Se atom substructures

As the popularity of the MAD method continues to grow (Ogata, 1998), there is a commensurate increase in the size of structures that are being tackled. In order to maintain an adequate anomalous scattering signal for larger macromolecules it is necessary to either increase the number of anomalous scatterers or incorporate heavier atoms. The exploitation of selenomethionyl proteins (Hendrickson, 1991; Doublie, 1997) provides an

Table 3

Examples of large selenium substructure determinations used in MAD phasing, for cases with more than 20 Se atoms.

| Structure | No. of Se atoms | Molecular weight (kDa) | Program | Reference |
|----------------------------|-----------------|------------------------|----------------------|-------------------------------|
| GPAase | 21 | 110 | <i>SnB/SHELX</i> | Kahn & Smith (1999) |
| E1b | 22 | 82 | <i>MR/Fourier</i> † | Ævarsson <i>et al.</i> (1999) |
| AdoMet decarboxylase | 24 | 76 | <i>SnB/SOLVE</i> | Ekstrom <i>et al.</i> (1999) |
| Napthalene-1,2-dioxygenase | 26 | 145 | <i>SIR/Fourier</i> ‡ | Kauppi <i>et al.</i> (1998) |
| PurR | 28 | 111 | <i>SHELX</i> | Sinha <i>et al.</i> (1998) |
| AIR synthetase | 28 | 148 | <i>SnB</i> | Li <i>et al.</i> (1999) |
| FTHF synthetase | 28 | 120 | <i>SHELX</i> | Lebioda <i>et al.</i> (1999) |
| FA hydrolase | 30 | 92 | <i>SOLVE</i> | Timm (1999) |
| AdoHcy hydrolase | 30 | 96 | <i>SnB</i> | Turner <i>et al.</i> (1998) |
| Cyanase | 40 | 170 | <i>CNS</i> | Walsh <i>et al.</i> (1999) |
| EphB2-SAM | 48 | 78 | <i>SnB</i> | Thanos <i>et al.</i> (1999) |
| AGM epimerase | 70 | 370 | <i>SnB</i> | Deacon <i>et al.</i> (1999) |

† Molecular replacement phases and Fourier techniques were used to locate the selenium substructure. ‡ Single isomorphous replacement phases and Fourier techniques were used to locate the selenium substructure.

intrinsically scalable approach to the MAD method, due to the natural abundance of methionine, amounting to approximately one in every 59 amino acid residues. However, for large proteins, locating the anomalous scattering atoms can then become a major hurdle in the phasing process. In the past, hand interpretation of Patterson maps has been the standard technique for locating a few anomalous scatterers. However, the use of Patterson techniques becomes more challenging with a larger number of sites. The application of automated and correlated Patterson searches, as implemented in the programs *CNS* (Brunger *et al.*, 1998) and *SOLVE* (Terwilliger *et al.*, 1987; Terwilliger & Berendzen, 1999), has been very successful in extending the range of Patterson techniques to larger structures. These programs have been used to resolve as many as 40 and 30 independent selenium sites, respectively (Table 3). Nevertheless, even these methods can be expected to break down as the number of sites continues to increase. In the case of a 70 Se-atom substructure, the Patterson maps are crowded and the Harker sections become littered with cross-vectors, as well as self-vectors (Fig. 5). An alternative approach, which has been recognized for some time, is in the use of direct methods. The isomorphous differences (Wilson, 1978; Adams *et al.*, 1977), anomalous differences (Mukherjee *et al.*, 1989) and dispersive differences (Evans & Wilson, 1999) have all been used. However, in these studies only a few anomalous scatterers were sought. For larger selenomethionine substructures any two Se atoms cannot be closer than ~ 4.0 Å, as dictated by the van der Waals radius for selenium. In practice, the average separation of two distinct methionine S atoms is ~ 7.5 Å and most structures have a closest S–S distance of the order of 6 Å. Therefore, the task still seems amenable to a direct-methods approach at 3.0 Å resolution. Moreover, the recent development of two robust dual-space direct-methods programs (Weeks *et al.*, 1996) now offers a choice of fast and automatic tools to locate the positions of extremely large anomalous scattering substructures. The first program, *SnB* (Weeks &

Miller, 1999), is based on the refinement of a minimal function (Hauptman, 1991). It has been used to solve entire structures as large as 1200 independent non-H atoms (Deacon *et al.*, 1998). It has also been extremely successful with several of the largest substructures in the 30–70 Se atom range (Table 3). The use of anomalous differences coupled with careful outlier rejection has so far been the key to success (Smith *et al.*, 1998; Blessing & Smith, 1999). The second program, *SHELXD* (Sheldrick, 1998), is in the latter stages of testing before general release, and has already been used to solve structures of more than 2000 atoms (Frazão *et al.*, 1999) and some large substructures (Table 3). In the light of these recent achievements it appears that the structure determination of large macromolecules and even macromolecular assemblies by a joint direct methods and MAD phasing protocol is now tenable.

4. MAD and technology/technique advances at ESRF

The use of MAD as a technique to solve the phase problem has hugely increased in recent years. The selenomethionine method (Hendrickson *et al.*, 1990) is becoming widely applicable. For example, in 1995, when the ESRF BM14 line opened, experimental proposals requesting MAD made up 30% of the requests for total beam time, whereas in September 1998 they made up 140%. Of the absorption edges used in 1998 on BM14 at ESRF, 18 were Se-met, three Fe, five Hg, one Yb, one Br, one W, two Pt and one Au. This increased use is based on several factors, all of which have contributed as follows:

(a) The growing awareness in the structural biology community of the quality of MAD electron density maps with no errors due to lack of isomorphism.

(b) The increasing availability of synchrotron beamlines capable of making the measurements.

(c) The decreasing amount of beam time required to make the measurements. With the advent of more powerful sources and faster detectors, a typical experiment nowadays

lasts less than 24 h and in some cases much less. [As described in §2.1, this is a critical improvement of ESRF BM14 over SRS station 9.5 beam-time needs for a MAD protein structure determination.]

(d) The increased simplicity of detector data processing, aided by the realization that MAD data could be successfully phased using a 'quasi MIR' approach culminating in the recent developments of structure solution program packages [see article by Fourme *et al.* (1999) in this issue].

(e) The possibility to cryoprotect samples and record data from a single crystal instead of having to scale many together.

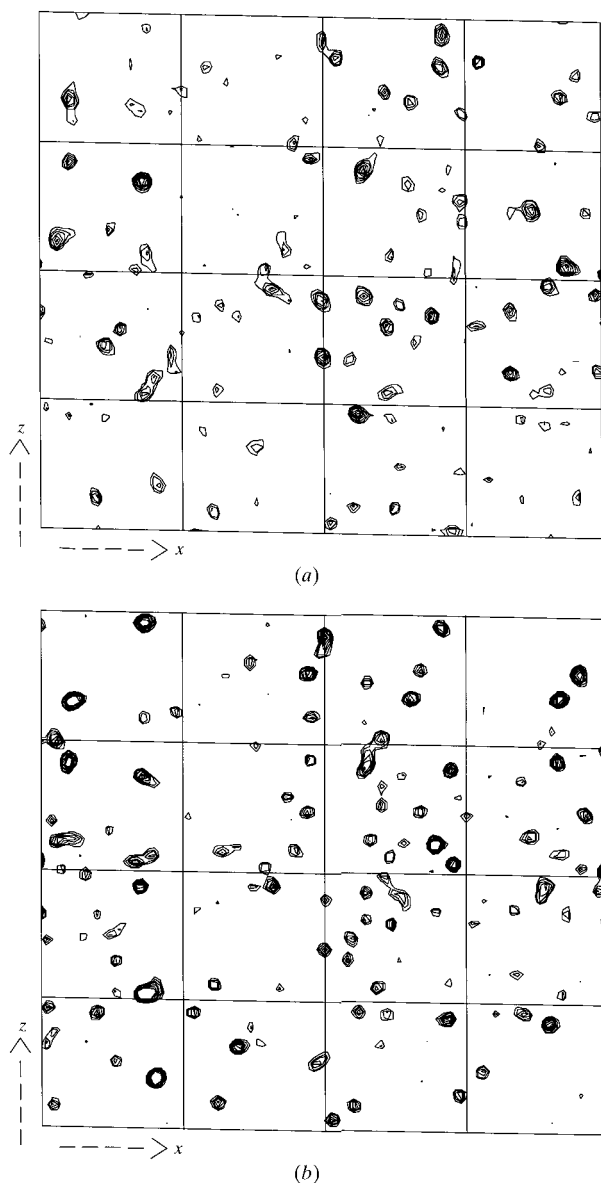


Figure 5
Patterson maps for ADP-L-glycero-D-mannoheptose 6-epimerase, containing 70 Se atoms. Harker section $y = 1/2$, with x from 0 to 1.0 and z from 0 to 0.5. Contours every 0.5σ starting at 2σ . (a) Observed anomalous difference Patterson map (based on 'peak' wavelength data set). (b) Calculated Patterson map based on the final coordinates set for the Se atoms.

Of course, the very technological advances that have helped the method will pose further challenges for the future. For example:

What is the best data-collection strategy for cryoprotected samples in a very intense third-generation synchrotron beam, where the sample radiation damage limit is reached in a few minutes of total exposure?

What are the possibilities that will be offered by the increased size of the anomalous signal available when 'white lines' are probed at higher energy resolution using a

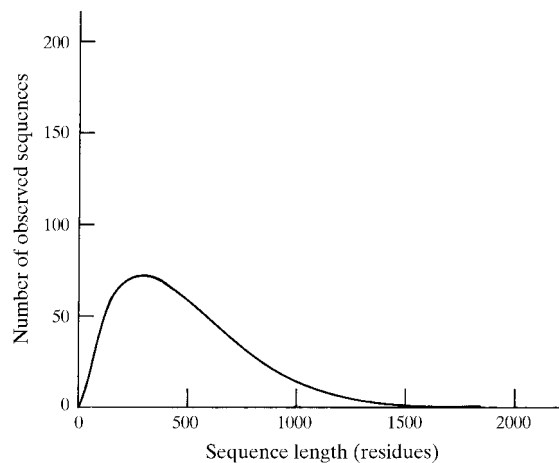


Figure 6
Histogram of protein molecular weights derived from the yeast genome. [Based on Das *et al.* (1997).]

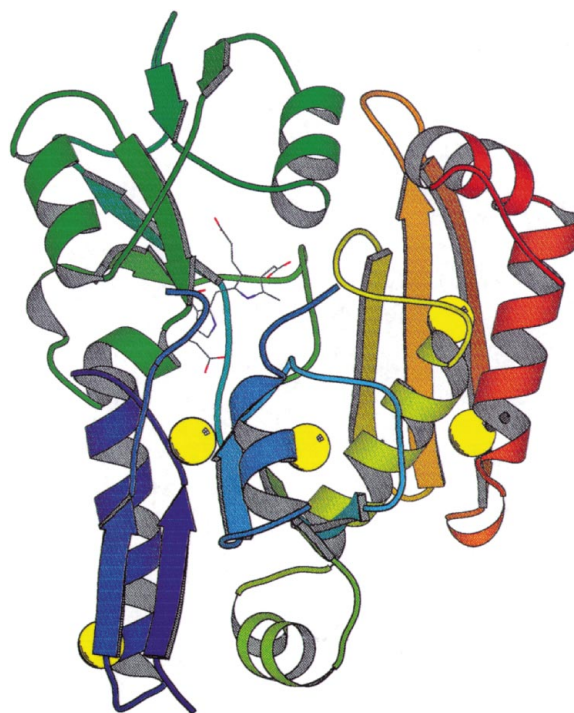


Figure 7
A representative example of Se-met protein crystal structures illustrating a typical molecular weight case (see Fig. 6). Hydroxymethylbilane synthase at SRS 9.5 involving five Se atoms in 34 kDa (Hädener *et al.*, 1999, with permission of IUCr).

high-brilliance ESRF undulator MAD beamline? This improvement could be as much as 30% for a single Se, allowing 'weaker' anomalous scattering signals to be measured. But will our beamlines be stable enough to take full advantage of this? What more information can we gain from the varying chemical environments that the heavy atoms experience, and how will this vary from crystal batch to crystal batch (Smith & Thompson, 1998)?

What new possibilities will be realised by improved detectors such as pixel detectors? Their fast readout will allow yet more efficient data collection on intense and tunable MAD beamlines.

What is the real limit of the size of small anomalous signals that can be useful in structure solution if signals as weak as 1.4% have already resulted in meaningful electron density maps?

What is the limit in terms of the size of structures that can be tackled by MAD, now that the 'many Se' problem is showing signs of cracking (as described in detail in §3)?

Structures have been solved on an ESRF dipole beamline in as little as 7.5 h (from mounting a crystal to interpretable electron density map). Automatic electron-density fitting programs are being developed to complement automatic phasing programs. How soon will structure determination become a totally automatic procedure? This has hugely important implications for synchrotron radiation facility development and policy.

5. Towards structural genomics

A number of whole organism gene sequences (genomes) are known today, and from which protein amino acid sequences are derived (the proteome equivalents). An idea of the general composition of a proteome is seen in Fig. 6, which shows the histogram of protein molecular weights derived from the yeast genome. This peaks at a protein molecular weight of 30 kDa. As an example of the distribution of Se atoms in a protein structure for this 'peak weight', see Fig. 7. Obviously, oligomeric proteins occur and they represent larger multimacromolecular complexes that will need to be solved crystallographically. The total number of proteins in a proteome varies between 10000 for the yeast to 100000 for the human proteome. Bioinformatic analysis seeks to use the amino acid sequences and compare against the known three-dimensional protein structures (with their amino acid sequences) and by homology seek to predict which proteins might represent 'new fold targets'. There are likely to develop then subsets of genomes of main interest for three-dimensional crystal structure analysis. The lessons from gene sequencing projects are, however, to seek to sequence *all* of a genome, which has yielded surprises (unknown proteins, *i.e.* with respect to function). A technical restriction will arise in that 40% of all the proteins in a genome are membrane-bound and much more difficult to crystallize than non-membrane-bound globular proteins. Even for the latter group of soluble proteins, protein crystal growth and protein

preparation are now the main rate-limiting steps for proteome level numbers of protein crystal structure determinations (Chayen & Helliwell, 1998). There is at least a factor of ten (even 100) mismatch between the MAD beam time needed (hours) *versus* the protein crystal growth time (days/weeks). A 'synchrotron radiation proteomics factory' would need many crystal sample preparation 'production lines' for it to be kept busy. The exploration of the functionality of proteins, as well as structures, is discussed in this issue by Ren *et al.* (1999) (see also Helliwell & Rentzepis, 1997).

This article has surveyed the development at four synchrotron radiation facilities. Worldwide, other developments have been ongoing obviously [*e.g.* Hendrickson, 1985, 1991, 1999 (this issue); Guss *et al.*, 1988; Kahn *et al.*, 1985; Fourme *et al.*, 1999 (this issue)].

Coordination between synchrotron radiation facilities to avoid duplication of protein structure determinations can readily be performed *via* the internet. This would require considerable openness and cooperation. A network of global synchrotron radiation PX stations, a global synchrotron radiation PX village, is feasible. The potential for rational drug design (*e.g.* see Ealick *et al.*, 1990; Bugg *et al.*, 1993) and the understanding of the molecular basis of disease is immense, rendering this a very important goal.

The facilities and machine staff at Daresbury, Cornell, ESRF and Trieste are thanked for fruitful collaborations over many years. AC thanks Drs A. Lausi and F. Zanini of Sincrotrone Trieste for their help. SEE and AMD would like to thank D. J. Thiel for discussions and providing Fig. 3 and J. L. Smith for information in Table 3. Research at CHESS is supported by grant DMR-9311772 from the National Science Foundation and the MacCHESS research resource is funded by grant RR-01646 from the National Institutes of Health. SEE and AMD would also like to acknowledge support of grant GM-46733 from the National Institutes of Health. JRH thanks the SERC, MRC and Swedish NFR for funding the SRS PX stations 7.2, 9.6 and 9.5 developments between 1979 and 1993 at Daresbury. JRH also wishes to thank BBSRC and EPSRC for research grant funding for utilization of SRS and ESRF for the MAD research projects at the University of Manchester; within these programmes fruitful collaborations with Dr A. Hädener, Dr W. N. Hunter and Dr G. A. Leonard are also gratefully acknowledged involving Se-methionine hydroxymethylbilane synthase and a brominated oligonucleotide. JRH warmly thanks Dr N. E. Chayen, Imperial College, London, for discussions on protein crystallization.

References

- Abrahams, J. P., Leslie, A. G. W., Lutter, R. & Walker, J. E. (1994). *Nature (London)*, **370**, 621–628.
- Acharya, R., Fry, E., Stuart, D., Fox, G., Rowlands, D. & Brown, F. (1989). *Nature (London)*, **337**, 709–716.

- Adams, M. J., Helliwell, J. R. & Bugg, C. E. (1977). *J. Mol. Biol.* **112**, 183–197.
- Ævarsson, A., Seger, K., Turley, S., Sokatch, J. R. & Hol, W. G. J. (1999). *Nat. Struct. Biol.* In the press.
- Arndt, U. W., Greenhough, T. J., Helliwell, J. R., Howard, J. A. K., Rule, S. A. & Thompson, A. W. (1982). *Nature (London)*, **298**, 835–838.
- Arndt, U. W. & Wonacott, A. J. (1977). *The Rotation Method in Crystallography*. Amsterdam: North Holland.
- Bailey, S., Smith, K., Fairlamb, A. H. & Hunter, W. N. (1993). *Eur. J. Biochem.* **213**, 67–75.
- Baker, P. J., Farrants, G. W., Stillman, T. J., Britton, K. L., Helliwell, J. R. & Rice, D. W. (1990). *Acta Cryst.* **A46**, 721–725.
- Bernstorff, S., Busetto, E., Gramaccioni, C., Lausi, A., Olivi, L., Zanini, F., Savoia, A., Colapietro, M., Portalone, G., Camalli, M., Pifferi, A., Spagna, R., Barba, L. & Cassetta, A. (1995). *Rev. Sci. Instrum.* **66**(2), 1661–1664.
- Bernstorff, S., Busetto, E., Savoia, A. & Colapietro, M. (1995). *Rev. Sci. Instrum.* **66**(2), 2065–2068.
- Blessing, R. H. & Smith, G. D. (1999). *J. Appl. Cryst.* In the press.
- Bourgeois, D., Ursby, T., Wulff, M., Pradervand, C., Legrand, A., Schildkamp, W., Laboure, S., Srajer, V., Teng, T. Y., Roth, M. & Moffat, K. (1996). *J. Synchrotron Rad.* **3**, 65–74.
- Brammer, R. C., Helliwell, J. R., Lamb, W., Liljas, A., Moore, P. R., Thompson, A. W. & Rathbone, K. (1988). *Nucl. Instrum. Methods*, **A271**, 678–687.
- Brunger, A. T., Adams, P. D., Clore, G. M., DeLano, W. L., Gros, P., Grosse-Kunstleve, R. W., Jiang, J.-S., Kuszewski, J., Nilges, M., Pannu, N. S., Read, R. J., Rice, L. M., Simonson, T. & Warren, G. L. (1998). *Acta Cryst.* **D54**, 905–921.
- Bugg, C. E., Carson, W. M. & Montgomery, J. A. (1993). *Sci. Am.* **12**, 60–66.
- Bujacz, G., Jaskoski, M., Alexandratos, J., Wlodawer, A., Merkel, G., Katz, R. A. & Skalka, A. M. (1995). *J. Mol. Biol.* **253**, 333–346.
- Chayen, N. & Helliwell, J. R. (1998). *Phys. World*, **5**, 43–48.
- Chayen, N. E., Boggon, T. J., Cassetta, A., Deacon, A., Gleichmann, T., Habash, J., Harrop, S. J., Helliwell, J. R., Nieh, Y. P., Peterson, M. R., Raftery, J., Snell, E. H., Hädener, A., Niemann, A. C., Siddons, D. P., Stojanoff, V., Thompson, A. W., Ursby, T. & Wulff, M. (1996). *Q. Rev. Biophys.* **29**(3), 227–278.
- Collaborative Computational Project, Number 4 (1994). *Acta Cryst.* **D50**, 760–763.
- Das, S., Yu, L. H., Gaitatzes, C., Rogers, R., Freeman, J., Bienkowska, J., Adams, R. M., Smith, T. F. & Lindellen, J. (1997). *Nature (London)*, **385**, 29–30.
- Deacon, A., Gleichmann, T., Kalb, A. J., Price, H., Raftery, J., Bradbrook, G., Yariv, J. & Helliwell, J. R. (1997). *J. Chem. Soc. Faraday Trans.* **93**(24), 4305–4312.
- Deacon, A., Habash, J., Harrop, S. J., Helliwell, J. R., Hunter, W. N., Leonard, G. A., Peterson, M., Hädener, A., Kalb, A. J., Allinson, N. M., Castelli, C., Moon, K., McSweeney, S., Gonzalez, A., Thompson, A. W., Ealick, S., Szebenyi, D. M. & Walter, R. (1995). *Rev. Sci. Instrum.* **66**(2), 1287–1292.
- Deacon, A. M., Ni, Y., Coleman, W. G. Jr & Ealick, S. E. (1999). Private communication.
- Deacon, A. M., Weeks, C. M., Miller, R. & Ealick, S. E. (1998). *Proc. Natl Acad. Sci. USA*, **95**, 9284–9289.
- Doublie, S. (1997). *Methods Enzymol.* **276**, 523–530.
- Duke, E. M. H., Kehoe, R. C., Rizkallah, P. J., Clarke, J. A. & Nave, C. (1998). *J. Synchrotron Rad.* **5**, 497–499.
- Ealick, S. E., Rule, S. A., Carter, D. C., Greenhough, T. J., Babu, Y. S., Cook, W. J., Habash, J., Helliwell, J. R., Stoeckler, J. D., Parks, R. E. Jr, Chen, S. & Bugg, C. E. (1990). *J. Biol. Chem.* **265**, 1812–1820.
- Einspahr, H., Suguna, K., Suddath, F. L., Ellis, G., Helliwell, J. R. & Papiz, M. Z. (1985). *Acta Cryst.* **B41**, 336–341.
- Ekstrom, J. L., Mathews, I. I., Stanley, B. A., Pegg, A. E. & Ealick, S. E. (1999). *Structure*, **7**, 583–595.
- Evans, G. & Wilson, K. S. (1999). *Acta Cryst.* **D55**, 67–76.
- Fourme, R., Shepard, W., Schiltz, M., Prangé, T., Ramin, M., Kahn, R., de la Fortelle, E. & Bricogne, G. (1999). *J. Synchrotron Rad.* **6**, 834–844.
- Frazaõ, C., Sieker, L., Sheldrick, G. M., Lamzin, V., LeGall, J. & Corondo, M. A. (1999). *J. Bioinorg. Chem.* In the press.
- Friedman, A. M., Fischmann, T. O. & Steitz, T. A. (1995). *Science*, **268**, 1721–1727.
- Glover, I. D., Denny, R. C., Nguti, N. D., McSweeney, S. M., Kinder, S. H., Thompson, A. W., Dodson, E. J., Wilkinson, A. J. & Tame, J. R. H. (1995). *Acta Cryst.* **D51**, 39–47.
- Greenhough, T. J. & Helliwell, J. R. (1982). *J. Appl. Cryst.* **15**, 493–508.
- Grimes, J. M., Jakana, J., Ghosh, M., Basak, A. K., Roy, P., Chiu, W., Stuart, D. I. & Prasad, B. V. V. (1997). *Structure*, **5**, 885–893.
- Guss, J. M., Merrit, E. A., Phizackerley, R. P., Hedman, B., Murata, M., Hodgson, K. O. & Freeman, H. C. (1988). *Science*, **241**, 806–811.
- Hädener, A., Matzinger, P. K., Battersby, A. R., McSweeney, S., Thompson, A. W., Hammersley, A. P., Harrop, S. J., Cassetta, A., Deacon, A., Hunter, W. N., Nieh, Y. P., Raftery, J., Hunter, N. & Helliwell, J. R. (1999). *Acta Cryst.* **D55**, 631–643.
- Haslegrove, J. C., Faruqi, A. R., Huxley, H. E. & Arndt, U. W. (1977). *J. Phys. E*, **10**, 1035–1044.
- Hasnain, S. S. & Hodgson, K. O. (1999). *J. Synchrotron Rad.* **6**, 852–864.
- Hauptman, H. A. (1995). *Crystallographic Computing 5: From Chemistry to Biology*, edited by D. Moras, A. D. Podjarny & J. C. Thierry, pp. 324–332. IUCr/Oxford University Press.
- Hedman, B., Hodgson, K. O., Helliwell, J. R., Liddington, R. & Papiz, M. Z. (1985). *Proc. Natl Acad. Sci. USA*, **82**, 7604–7607.
- Helliwell, J. R. (1977a). *New Sci.* **76**, 646–648.
- Helliwell, J. R. (1977b). DPhil thesis, Oxford University, UK.
- Helliwell, J. R. (1979). *Proceedings of Daresbury Study Weekend*, DL/Sci/R13, pp. 1–6, 26–28 January 1979. Warrington: Daresbury Laboratory.
- Helliwell, J. R. (1984). *Rep. Prog. Phys.* **47**, 1403–1497.
- Helliwell, J. R. (1985). *J. Mol. Struct.* **130**, 63–91.
- Helliwell, J. R. (1987). ESRF Foundation Phase Report. ESRF, Grenoble, France.
- Helliwell, J. R. (1992). *Macromolecular Crystallography with Synchrotron Radiation*. Cambridge University Press.
- Helliwell, J. R. (1998). *Nat. Struct. Biol. (Synchrotron Suppl.)*, pp. 614–617.
- Helliwell, J. R., Cruickshank, D. W. J., Ellis, G., Habash, J., Papiz, M. Z. & Rule, S. A. (1984). *Proceedings of Daresbury Study Weekend*, DL/Sci/R22, pp. 41–59. Warrington: Daresbury Laboratory.
- Helliwell, J. R. & Fourme, R. (1983). Report to ESRP, Geneva.
- Helliwell, J. R., Greenhough, T. J., Carr, P., Rule, S. A., Moore, P. R., Thompson, A. W. & Worgan, J. S. (1982). *J. Phys. E*, **15**, 1363–1372.
- Helliwell, J. R., Papiz, M. Z., Glover, I. D., Habash, J., Thompson, A. W., Moore, P. R., Harris, N., Croft, D. & Pantos, E. (1986). *Nucl. Instrum. Methods*, **A246**, 617–623.
- Helliwell, J. R. & Rentzepis, P. M. (1997). Editors. *Time-Resolved Diffraction*. Oxford University Press.
- Helliwell, M., Helliwell, J. R., Kaucic, V., Zabukovec Logar, N., Barba, L., Busetto, E. & Lausi, A. (1999). *Acta Cryst.* **B55**, 327–332.
- Hendrickson, W. A. (1985). *Trans. Am. Cryst. Assoc.* **21**, 11–21.
- Hendrickson, W. A. (1991). *Science*, **254**, 51–58.
- Hendrickson, W. A. (1999). *J. Synchrotron Rad.* **6**, 845–851.
- Hendrickson, W. A., Horton, J. R. & Lemaster, D. M. (1990). *EMBO J.* **9**(5), 1665–1672.
- Herzenberg, A. & Lau, H. S. M. (1967). *Acta Cryst.* **22**, 24–28.

- Hope, H. (1988). *Acta Cryst.* **B44**, 22–26.
- Hoppe, W. & Jakubowski, U. (1975). *Anomalous Scattering*, edited by S. Ramaseshan & S. C. Abrahams, pp. 437–461. Copenhagen: Munksgaard.
- Hunter, N. S., Gleichmann, T. J., Helliwell, M., Barba, L., Busetto, E., Lausi, A., Price, H. J. & Helliwell, J. R. (1999). *Croat. Chem. Acta*. In the press.
- Kahn, J. M. & Smith, J. L. (1999). Private communication.
- Kahn, R., Fourme, R., Bosshard, R., Chiadmi, M., Risler, J. L., Dideberg, O. & Wery, J. P. (1985). *FEBS Lett.* **179**(1), 133–137.
- Kalb, A. J., Habash, J., Hunter, N. S., Price, H. J., Raftery, J. & Helliwell, J. R. (1999). *Metals Biol.* **37**. In the press.
- Kauppi, B., Lee, K., Carredano, E., Parales, R. E., Gibson, D. T., Eklund, H. & Ramaswamy, S. (1998). *Structure*, **6**, 571–586.
- Laboure, S., Leonard, G., Stojanoff, V., Svensson, O. & Thompson, A. W. (1999). *ESRF Annual Reports and Highlights*. ESRF, Grenoble, France.
- Leahy, D. J., Hendrickson, W. A., Aukhil, I. & Erickson, H. P. (1992). *Science*, **258**, 987–991.
- Lebioda, L., Radfar, R., Shin, R., Sheldrick, G. M., Odom, J. D. & Dunlap, R. B. (1999). Personal communication.
- Lemonnier, M., Fourme, R., Rousseaux, F. & Kahn, R. (1978). *Nucl. Instrum. Methods*, **152**, 173–177.
- Li, C., Kappock, T. J., Stubbe, J. & Ealick, S. E. (1999). *Structure*. In the press.
- Liddington, R. C., Yan, Y., Moulai, J., Sahli, R., Benjamin, T. L. & Harrison, S. C. (1991). *Nature (London)*, **354**, 278–284.
- Mukherjee, A., Helliwell, J. R. & Main, P. (1989). *Acta Cryst.* **A45**, 715–718.
- Newman, M., Strzelecka, T., Domer, L. F., Schildkraut, I. & Aggarwal, A. K. (1994). *Nature (London)*, **368**, 660–664.
- Nieh, Y. P. & Helliwell, J. R. (1995). *J. Synchrotron Rad.* **2**, 79–82.
- Ogata, C. M. (1998). *Nat. Struct. Biol. (Synchrotron Suppl.)*, **5**, 638–640.
- Okaya, Y. & Pepinsky, R. (1956). *Phys. Rev.* **103**, 1645.
- Peterson, M. R., Harrop, S. J., McSweeney, S. M., Leonard, G. A., Thompson, A. W., Hunter, W. N. & Helliwell, J. R. (1996). *J. Synchrotron Rad.* **3**, 24–34.
- Ren, Z., Bourgeois, D., Helliwell, J. R., Srajer, V., Stoddard, B. L. & Moffat, K. (1999). *J. Synchrotron Rad.* **6**, 891–917.
- Rizkallah, P. J. (1999). *Protein Crystallography Publications*, <http://www.dl.ac.uk/SRS/PX/publications.html>.
- Rodgers, D. W. (1994). *Structure*, **2**, 1135–1140.
- Rossmann, M. G. (1999). *J. Synchrotron Rad.* **6**, 816–821.
- Shamoo, Y., Friedman, A. M., Parsons, M. R., Konigsberg, W. H. & Steitz, T. A. (1995). *Nature (London)*, **376**, 362–366.
- Sheldrick, G. M. (1998). *Direct Methods for Solving Structures*, edited by S. Fortier, pp. 401–411. Dordrecht: Kluwer.
- Sinha, S., Krahn, J. M., Shin, B. S., Tomchick, D. R., Zalkin, H. & Smith, J. L. (1998). ACA Meeting, Arlington, 18–23 July 1998. W0012.
- Smith, G. D., Nagar, B., Rini, J. M., Hauptman, H. A. & Blessing, R. H. (1998). *Acta Cryst.* **D54**, 799–804.
- Smith, J. L. & Thompson, A. W. (1998). *Structure*, **6**(7), 815–819.
- Smolenski, K. W., Shen, Q. & Doing, P. (1997). *Proc. SPIE*, **3151**, 181–187.
- Szebenyi, D. M. E., Arvai, A., Ealick, S., LaIuppa, J. M. & Nielsen, C. (1997). *J. Synchrotron Rad.* **4**, 128–135.
- Tate, M. R., Eikenberry, E. F., Barna, S. L., Wall, M. E., Lawrence, J. L. & Gruner, S. M. (1995). *J. Appl. Cryst.* **28**, 196–205.
- Teng, T. Y. (1990). *J. Appl. Cryst.* **23**, 387–391.
- Terwilliger, T. C. & Berendzen, J. (1999). *Acta Cryst.* In the press.
- Terwilliger, T. C., Kim, S.-H. & Eisenberg, D. (1987). *Acta Cryst.* **A43**, 1–5.
- Thanos, C. D., Goodwill, K. E. & Bowie, J. U. (1999). *Science*, **282**, 833–836.
- Thiel, D. J., Blank, B. & LaIuppa, J. (1998). *J. Synchrotron Rad.* **5**, 914–916.
- Thiel, D. J., Ealick, S. E., Tate, M. W., Gruner, S. M. & Eikenberry, E. F. (1996). *Rev. Sci. Instrum.* **67**, 1.
- Thiel, D. J., le Du, M., Walter, R. L., D'Arcy, A., Chene, C., Fontoulakis, M., Garotta, G., Winkler, F. & Ealick, S. E. (1995). *5th International Conference on Biophysics and Synchrotron Radiation*, Grenoble, France. Abstract 01/38.
- Thompson, A. W., Habash, J., Harrop, S., Helliwell, J. R., Nave, C., Atkinson, P., Hasnain, S. S., Glover, I. D., Moore, P. R., Harris, N., Kinder, S. & Buffey, S. (1992). *Rev. Sci. Instrum.* **63**(1), 1062–1064.
- Timm, D. E. (1999). Private communication.
- Todd, A. K., Adams, A., Powell, H. R., Wilcock, D. J., Thorpe, J. H., Lausi, A., Zanini, F., Wakelin, L. P. G. & Cardin, C. J. (1999). *Acta Cryst.* **D55**, 729–735.
- Turner, M. A., Yuan, C.-S., Borchardt, R. T., Hershfield, M. S., Smith, G. D. & Howell, P. L. (1998). *Nat. Struct. Biol.* **5**, 369–376.
- Wakatsuki, S., Belrhali, H., Mitchell, E. P., Burmeister, W. P., McSweeney, S. M., Kahn, R., Bourgeois, D., Yao, M., Tomizaki, T. & Theveneau, P. (1998). *J. Synchrotron Rad.* **5**, 215–221.
- Walsh, M. A., Otwinowski, Z., Perrakis, A., Anderson, P. M. & Joachimiak, A. (1999). Private communication.
- Walter, R. L., Ealick, S. E., Friedman, A. M., Blake, R. C., Proctor, P. & Shoham, M. (1996). *J. Mol. Biol.* **263**, 730–751.
- Walter, R. L., Thiel, D. J., Barna, S. L., Tate, M. W., Eikenberry, E. F., Gruner, S. M. & Ealick, S. E. (1995). *Structure*, **3**, 835–844.
- Weeks, C. M. & Miller, R. (1999). *J. Appl. Cryst.* **32**, 120–124.
- Weeks, C. M., Sheldrick, G. M., Miller, R., Uson, I. & Hauptman, H. A. (1999). *Bull. Czech Slovak Crystallogr. Assoc.* In the press.
- Wilson, K. S. (1978). *Acta Cryst.* **A45**, 718–726.